Performance Analysis of Godard-Based Blind Channel Identification

Philip Schniter
The Ohio State University
Columbus, OH 43210 USA
schniter@ee.cornell.edu

Abstract

We analyze a blind channel impulse response identification scheme based on the cross-correlation of blind symbol estimates with the received signal. The symbol estimates specified are those minimizing the Godard (or constant modulus) criterion, for which mean-squared symbol estimation error bounds have recently been derived. In this paper, we derive upper bounds for the average squared parameter estimation error of the blind identification scheme which depend on the mean-squared error of Wiener symbol estimator, the kurtoses of the desired and interfering sources, and the channel impulse response. All results are derived in a general multi-user vector-channel context.

1.0 Introduction

Consider the linear system of Fig. 1, where a desired source sequence $\{s_n^{(0)}\}$ combines linearly with K interferers through vector channels $\{\mathbf{h}^{(0)}(z), \ldots, \mathbf{h}^{(K)}(z)\}$. Our goal is to estimate the impulse response coefficients of the linear channel $\{\mathbf{h}^{(0)}(z)\}$ knowing only the statistics of the received signal $\{\mathbf{r}_n\}$. The literature refers to this problem as *blind* channel identification [1].

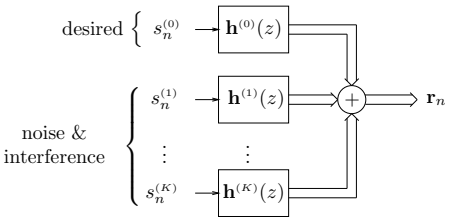

Fig. 1. Multi-source linear system model.

In this paper, we analyze the performance of the blind channel identification scheme illustrated in Fig. 2, whereby blind symbol estimates $\{y_n\}$ are cross-correlated with the received signal $\{\mathbf{r}_n\}$ under the presumption that the source processes $\{s_n^{(0)}\} \ldots \{s_n^{(K)}\}$ are mutually independent. We focus specifically on the case of blind linear symbol estimates minimizing the Godard, or constant modulus (CM), criterion [2], [3], [4].

Minimization of the CM criterion has become perhaps the most studied and implemented means of blind symbol estimation for data communication over dispersive channels (see, e.g., [4] and the references within). The popularity of CM methods are usually attributed to

1. the existence of a simple adaptive algorithm ("CMA" [2], [3]) for estimation and tracking of the CM-minimizing linear estimator $\mathbf{f}_{\mathrm{c},\nu}(z)$,
2. the typically excellent mean-squared error (MSE) performance of CM-minimizing estimator [6], and
3. the insensitivity to residual carrier phase/frequency offsets in received signal $\mathbf{r}_n$.

In this paper, we derive upper bounds for the average squared parameter error (ASPE) of blind channel parameter estimates generated by the method of Fig. 2. We also derive the expected ASPE that results when the correlations in Fig. 2 are estimated from N-length blocks of data.

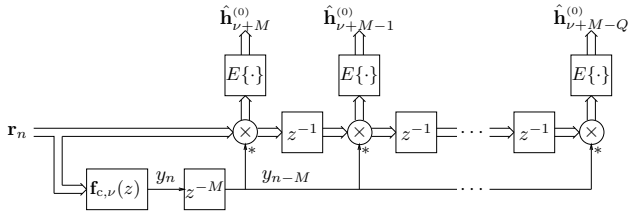

Fig. 2. CM-based blind channel identification.

2.0 Background

The following notation is used throughout: $(\cdot)^t$ denotes transpose, $(\cdot)^*$ conjugation, $(\cdot)^H$ hermitian, $\mathrm{E}\{\cdot\}$ denotes expectation, and $\|\mathbf{x}\|_p$ the p-norm defined by $\sqrt[p]{\sum_i |x_i|^p}$. In general, we use boldface lowercase type to denote vector quantities and boldface uppercase type to denote matrix quantities.

2.1 Linear System Model

First we formalize the linear time-invariant multi-channel model illustrated in Fig. 1. Say that the de-

sired symbol sequence $\{s_n^{(0)}\}$ and K sources of interference $\{s_n^{(1)}\},\ldots,\{s_n^{(K)}\}$ each pass through separate linear channels before being observed. In addition, say that the symbol estimator uses a sequence of P-dimensional vector observations $\{\mathbf{r}_n\}$ to estimate (a possibly delayed version of) the desired source sequence, where the case $P>1$ corresponds to the use of multiple sensors and/or sampling at an integer multiple of the symbol rate. The observations can be written $\mathbf{r}_n=\sum_{k=0}^{K}\sum_{i=0}^{\infty}\mathbf{h}_i^{(k)}s_{n-i}^{(k)}$, where $\{\mathbf{h}_n^{(k)}\}$ denote the impulse response coefficients of the linear time-invariant (LTI) channel $\mathbf{h}^{(k)}(z)$. The only assumptions placed on $\mathbf{h}^{(k)}(z)$ are causality and bounded-input bounded-output (BIBO) stability.

As shown in Fig. 2, linear estimates $\{y_n\}$ of $\{s_{n-\nu}^{(k)}\}$, for fixed estimation delay ν, are generated from the vector-valued observation sequence $\{\mathbf{r}_n\}$. Using $\{\mathbf{f}_n\}$ to denote the impulse response of the linear estimator $\mathbf{f}(z)$, the estimates are written as $y_n=\sum_{i=-\infty}^{\infty}\mathbf{f}_i^H\mathbf{r}_{n-i}$. We will assume that the linear system $\mathbf{f}(z)$ is BIBO stable with constraints on the number of adjustable parameters.

Often used in the sequel are the combined channel-plus-estimator "global" responses $q^{(k)}(z):=\mathbf{f}^H(z)\mathbf{h}^{(k)}(z)$. The impulse response coefficients of $q^{(k)}(z)$ are

$$q_n^{(k)} \;=\; \sum_{i=-\infty}^{\infty}\mathbf{f}_i^H\mathbf{h}_{n-i}^{(k)}, \tag{1}$$

allowing the estimates to be written as $y_n=\sum_k\sum_i q_i^{(k)}s_{n-i}^{(k)}$. Adopting the following vector notation helps to streamline the remainder of the paper.

$$\begin{aligned}\boldsymbol{q}&:=(\cdots,q_{-1}^{(0)},\ldots,q_{-1}^{(K)},q_0^{(0)},\ldots,q_0^{(K)},q_1^{(0)},\ldots,q_1^{(K)},\cdots)^t,\\ \boldsymbol{s}(n)&:=(\cdots,s_{n+1}^{(0)},\ldots,s_{n+1}^{(K)},s_n^{(0)},\ldots,s_n^{(K)},s_{n-1}^{(0)},\ldots,s_{n-1}^{(K)},\cdots)^t.\end{aligned}$$

For instance, we can concisely write $y_n=\boldsymbol{q}^t\boldsymbol{s}(n)$.

It is important to recognize that that placing a particular structure on the channel and/or estimator will restrict the set of *attainable* global responses, which we will denote by $\mathcal{Q}_{\rm a}$. For example, when the estimator is FIR, (1) implies that $\boldsymbol{q}\in\mathcal{Q}_{\rm a}=\mathrm{row}(\boldsymbol{\mathcal{H}})$, where

$$\boldsymbol{\mathcal{H}}:=\begin{pmatrix}\mathbf{h}_0^{(0)}\cdots\mathbf{h}_0^{(K)}&\mathbf{h}_1^{(0)}\cdots\mathbf{h}_1^{(K)}&\mathbf{h}_2^{(0)}\cdots\mathbf{h}_2^{(K)}&\cdots\\ \mathbf{0}\;\cdots\;\mathbf{0}&\mathbf{h}_0^{(0)}\cdots\mathbf{h}_0^{(K)}&\mathbf{h}_1^{(0)}\cdots\mathbf{h}_1^{(K)}&\cdots\\ \vdots\quad\vdots&\vdots\quad\vdots&\vdots\quad\vdots&\\ \mathbf{0}\;\cdots\;\mathbf{0}&\mathbf{0}\;\cdots\;\mathbf{0}&\mathbf{h}_0^{(0)}\cdots\mathbf{h}_0^{(K)}&\cdots\end{pmatrix} \tag{2}$$

Restricting the estimator to be causal IIR, for example, would generate a different attainable set $\mathcal{Q}_{\rm a}$. In general, we allow any channel/estimator restrictions which ensure that $\mathcal{Q}_{\rm a}$ is a linear subspace of $\ell_1(\mathbb{C})$.

Throughout the paper, we make the following assumptions on the $K+1$ source processes:

S1) For all k, $\{s_n^{(k)}\}$ is zero-mean i.i.d.
S2) $\{s_n^{(0)}\}\cdots\{s_n^{(K)}\}$ are jointly independent.
S3) For all k, $\mathrm{E}\{|s_n^{(k)}|^2\}=\sigma_s^2$.
S4) $\mathcal{K}(s_n^{(0)})<0$, where $\mathcal{K}(\cdot)$ denotes kurtosis:

$$\mathcal{K}(s_n) \;:=\; \mathrm{E}\{|s_n|^4\}-2\big(\mathrm{E}\{|s_n|^2\}\big)^2-\big|\mathrm{E}\{s_n^2\}\big|^2. \tag{3}$$

S5) If, for any k, $q^{(k)}(z)$ or $\{s_n^{(k)}\}$ is not real-valued, then $\mathrm{E}\{{s_n^{(k)}}^2\}=0$ for all k.

2.2 The Constant Modulus Criterion

The CM (or Godard) criterion, introduced independently in [2], [3], is defined as

$$J_{\rm c}(y_n) \;:=\; \mathrm{E}\big\{\big(|y_n|^2-\gamma\big)^2\big\}. \tag{4}$$

γ is a positive design parameter. We quantify the MSE performance of the CM estimator below.

Since both symbol power and channel gain are unknown in the "blind" scenario, blind estimates suffer from a gain ambiguity. To ensure that estimator performance evaluation is meaningful in the face of such ambiguity, we consider normalized versions of the estimates with normalization factor $q_\nu^{(0)}$. Given that the estimate y_n can be decomposed into signal and interference terms

$$y_n \;=\; q_\nu^{(0)}s_{n-\nu}^{(0)}+\bar{\boldsymbol{q}}^t\bar{\boldsymbol{s}}(n), \tag{5}$$

where $\bar{\boldsymbol{q}}$ denotes $\boldsymbol{q}$ with the $q_\nu^{(0)}$ term removed and $\bar{\boldsymbol{s}}(n)$ denotes $\boldsymbol{s}(n)$ with the $s_{n-\nu}^{(0)}$ term removed, the normalized estimate $y_n/q_\nu^{(0)}$ can be referred to as "conditionally unbiased" since $\mathrm{E}\{y_n/q_\nu^{(0)}|s_{n-\nu}^{(0)}\}=s_{n-\nu}^{(0)}$. The conditionally unbiased MSE (UMSE) associated with y_n, an estimate of $s_{n-\nu}^{(0)}$, is then defined

$$J_{{\rm u},\nu}(y_n) \;:=\; \mathrm{E}\big\{|y_n/q_\nu^{(0)}-s_{n-\nu}^{(0)}|^2\big\}. \tag{6}$$

Substituting (5) into (6), the UMSE becomes

$$J_{{\rm u},\nu}(\boldsymbol{q}) \;=\; \frac{\mathrm{E}\big\{|\bar{\boldsymbol{q}}^t\bar{\boldsymbol{s}}(n)|^2\big\}}{|q_\nu^{(0)}|^2} \;=\; \frac{\|\bar{\boldsymbol{q}}\|_2^2}{|q_\nu^{(0)}|^2}\,\sigma_s^2, \tag{7}$$

where the second equality invokes assumptions S1)–S3).

Henceforth we use $\boldsymbol{q}_{{\rm m},\nu}$ to denote the minimum-MSE (MMSE) global response associated with symbol delay ν. For the linear channel model of Fig. 1, it is possible to upper bound the UMSE of CM-minimizing symbol estimators of delay ν directly in terms of the UMSE of Wiener symbol estimators of the same delay, i.e., $J_{{\rm u},\nu}(\boldsymbol{q}_{{\rm m},\nu})$.

First we present some useful definitions. *Normalized* kurtosis κ (not to be confused with $\mathcal{K}(\cdot)$ in (3)) is

$$\kappa_s^{(k)} \;:=\; \frac{\mathrm{E}\big\{|s_n^{(k)}|^4\big\}}{\big(\mathrm{E}\{|s_n^{(k)}|^2\}\big)^2}. \tag{8}$$

Under the following definition of κ_g our results will hold for both real-valued and complex-valued models.

$$\kappa_g \;:=\; \begin{cases} 3, & \forall k,n:\ \mathbf{h}_n^{(k)} \in \mathbb{R}^P \text{ and } s_n^{(k)} \in \mathbb{R}, \\ 2, & \text{otherwise,} \end{cases} \tag{9}$$

Note that, under S1) and S5), κ_g represents the normalized kurtosis of a Gaussian source. The following quantities are also used in the sequel:

$$\kappa_s^{\min} := \min_{0\le k\le K} \kappa_s^{(k)}, \qquad \kappa_s^{\max} := \max_{0\le k\le K} \kappa_s^{(k)},$$
$$\rho_{\min} := \tfrac{\kappa_g-\kappa_s^{\min}}{\kappa_g-\kappa_s^{(0)}}, \qquad \rho_{\max} := \tfrac{\kappa_g-\kappa_s^{\max}}{\kappa_g-\kappa_s^{(0)}}.$$

Theorem 1 ([6]) *If* $J_{\mathrm{u},\nu}(\boldsymbol{q}_{\mathrm{m},\nu}) \le J_{\mathrm{o}}\sigma_s^2$, *where*

$$J_{\mathrm{o}} \;=\; \begin{cases} \sqrt{\frac{1+\rho_{\min}}{\rho_{\min}}} - 1 & \kappa_s^{\max} \le \kappa_g \\ \frac{1}{\rho_{\min}+\sqrt{(\rho_{\min}+1)(\rho_{\min}-\rho_{\max})}} & \kappa_s^{\max} > \kappa_g, \end{cases} \tag{10}$$

then the UMSE of CM-minimizing estimators associated[1] *with delay* ν *can be bounded as follows:*

$$J_{\mathrm{u},\nu}(\boldsymbol{q}_{\mathrm{m},\nu}) \;\le\; J_{\mathrm{u},\nu}(\boldsymbol{q}_{\mathrm{c},\nu}) \;\le\; J_{\mathrm{u},\nu}\big|_{\mathrm{c},\nu}^{\max},$$

where

$$J_{\mathrm{u},\nu}\big|_{\mathrm{c},\nu}^{\max}/\sigma_s^2 := \tag{11}$$
$$\begin{cases} \dfrac{1-\sqrt{(1+\rho_{\min})\left(1+\frac{J_{\mathrm{u},\nu}(\boldsymbol{q}_{\mathrm{m},\nu})}{\sigma_s^2}\right)^{-2}-\rho_{\min}}}{\rho_{\min}+\sqrt{(1+\rho_{\min})\left(1+\frac{J_{\mathrm{u},\nu}(\boldsymbol{q}_{\mathrm{m},\nu})}{\sigma_s^2}\right)^{-2}-\rho_{\min}}} & \text{when } \kappa_s^{\max} \le \kappa_g, \\ \dfrac{1-\sqrt{(1+\rho_{\min})\left(1+\frac{J_{\mathrm{u},\nu}(\boldsymbol{q}_{\mathrm{m},\nu})}{\sigma_s^2}\right)^{-2}\left(1+\rho_{\max}\frac{J^2_{\mathrm{u},\nu}(\boldsymbol{q}_{\mathrm{m},\nu})}{\sigma_s^4}\right)-\rho_{\min}}}{\rho_{\min}+\sqrt{(1+\rho_{\min})\left(1+\frac{J_{\mathrm{u},\nu}(\boldsymbol{q}_{\mathrm{m},\nu})}{\sigma_s^2}\right)^{-2}\left(1+\rho_{\max}\frac{J^2_{\mathrm{u},\nu}(\boldsymbol{q}_{\mathrm{m},\nu})}{\sigma_s^4}\right)-\rho_{\min}}} & \text{when } \kappa_s^{\max} > \kappa_g. \end{cases}$$

It should be noted that Theorem 1 implicitly incorporates the channel and/or estimator constraints that define $\mathcal{Q}_{\mathrm{a}}$ through its use of the MMSE response $\boldsymbol{q}_{\mathrm{m},\nu}(\in \mathcal{Q}_{\mathrm{a}})$. For example, if $\boldsymbol{q}_{\mathrm{m},\nu}$ is the MMSE global response constrained to the set of causal IIR estimators, then the UMSE bound pertains to CM-minimizing responses $\boldsymbol{q}_{\mathrm{c},\nu}$ obeying the same causal-IIR constraint.

2.3 Channel Identification

Fig. 2 illustrates the proposed blind channel impulse response identification scheme, whereby M-delayed versions of the CM-minimizing symbol estimates $\{y_n\} \approx \{s_{n-\nu}^{(0)}\}$ are cross-correlated with the vector received samples $\{\mathbf{r}_{n-Q},\ldots,\mathbf{r}_n\}$, yielding the channel parameter estimates $\{\hat{\mathbf{h}}_{\nu+M-Q}^{(0)},\ldots,\hat{\mathbf{h}}_{\nu+M}^{(0)}\}$. The δ^{th} parameter estimate $\hat{\mathbf{h}}_{\nu+M-\delta}^{(0)}$ can be expressed as a biased version of the true parameter corrupted by an error term:

$$\begin{aligned} \hat{\mathbf{h}}_{\nu+M-\delta}^{(0)} &= \mathrm{E}\left\{\mathbf{r}_{n-\delta}y_{n-M}^*\right\} \\ &= \mathrm{E}\Big\{\sum_{k,j}\mathbf{h}_j^{(k)}s_{n-\delta-j}^{(k)}\sum_{\ell,i}q_i^{(\ell)*}s_{n-M-i}^{(\ell)*}\Big\} \\ &= \sigma_s^2\sum_{k,i}\mathbf{h}_{i+M-\delta}^{(k)}\,q_i^{(k)*} \qquad (12) \\ &= \underbrace{\sigma_s^2\,q_\nu^{(0)*}}_{\text{bias}}\Bigg(\mathbf{h}_{\nu+M-\delta}^{(0)} + \underbrace{\sum_{(k,i)\neq(0,\nu)}\mathbf{h}_{i+M-\delta}^{(k)}\,\frac{q_i^{(k)*}}{q_\nu^{(0)*}}}_{\text{error}}\Bigg). \end{aligned}$$

The identification scheme in Fig. 2 bears similarity to the Gooch-Harp method of channel identification [7] illustrated in Fig. 3, whereby the CM-minimizing estimates $\{y_n\}$ are processed by a hard decision device $\mathcal{D}$ before cross-correlation. Due to the nonlinear operation $\mathcal{D}$, however, performance analysis of the Gooch-Harp scheme is difficult unless perfect decision-making (i.e., $d_n = s_{n-\nu}$) is assumed. In addition, forming reliable decisions requires carrier phase synchronization (an issue with passband data transmission) which is not required in the identification scheme of Fig. 2. (See [5].)

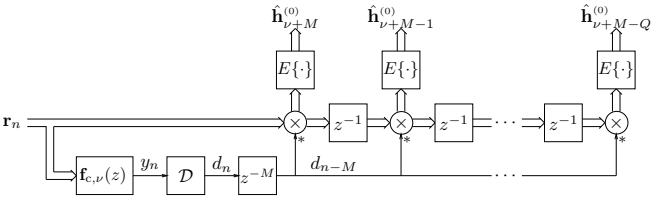

Fig. 3. Gooch & Harps' blind channel identification.

Many other methods of blind channel identification have been proposed [1], most of which estimate channel coefficients from the observed data directly, i.e., without first forming blind symbol estimates. When $P > 1$ and the channel satisfies certain conditions, it is possible to accomplish blind identification using only the second-order statistics (SOS) of the observed process Many SOS-based techniques, however, fail catastrophically when the channel order is incorrectly estimated. The CM-based schemes in Figs. 2 and 3, however, do not rely on the satisfaction of any channel-identifiability conditions.

[1] A CM-minimizing estimator is said to be *associated* with symbol delay ν when its global response $\boldsymbol{q}$ satisfies $|q_\nu^{(0)}| \ge \max_{(k,\delta)\neq(0,\nu)}|q_\delta^{(k)}|$ [6].

3.0 Blind Identification Performance

3.1 ASPE with Exact Correlations

We are interested in quantifying the average squared error of the parameter estimates $\{\hat{\mathbf{h}}^{(0)}_{\nu+M-Q},\ldots,\hat{\mathbf{h}}^{(0)}_{\nu+M}\}$ relative to the true parameters $\{\mathbf{h}^{(0)}_{\nu+M-Q},\ldots,\mathbf{h}^{(0)}_{\nu+M}\}$. We tolerate arbitrary scaling of the total estimated channel response and define our average squared parameter error (ASPE) criterion as follows.

$$\mathcal{E}_{\hat{\boldsymbol{h}}} \;:=\; \min_{\theta\in\mathbb{C}} \frac{1}{Q+1}\sum_{\delta=0}^{Q}\left\|\theta\,\hat{\mathbf{h}}^{(0)}_{\nu+M-\delta}-\mathbf{h}^{(0)}_{\nu+M-\delta}\right\|_2^2 \quad (13)$$

$$=\; \min_{\theta\in\mathbb{C}} \frac{1}{Q+1}\left\|\theta\underbrace{\begin{pmatrix}\hat{\mathbf{h}}^{(0)}_{\nu+M}\\ \vdots \\ \hat{\mathbf{h}}^{(0)}_{\nu+M-Q}\end{pmatrix}}_{\hat{\boldsymbol{h}}^{(0)}_{\nu+M}}-\underbrace{\begin{pmatrix}\mathbf{h}^{(0)}_{\nu+M}\\ \vdots \\ \mathbf{h}^{(0)}_{\nu+M-Q}\end{pmatrix}}_{\boldsymbol{h}^{(0)}_{\nu+M}}\right\|_2^2 \quad (14)$$

Note that by choosing M and Q large enough, an arbitrarily large subset of the total channel response $\mathbf{h}^{(0)}(z)$ may be estimated regardless of the symbol estimation delay ν.

Theorem 2: For symbol estimation delay ν, the ASPE generated by the blind channel identification scheme in Fig. 2 can be upper bounded as

$$\mathcal{E}_{\hat{\boldsymbol{h}}} \;\le\; \frac{\|\boldsymbol{\mathcal{H}}_M\|^2\, J_{\mathrm{u},\nu}\big|^{\max}_{\mathrm{c},\nu}}{(Q+1)\sigma_s^2} \;\le\; \frac{\mathrm{E}\left\{\|\mathbf{r}_n\|_2^2\right\}\, J_{\mathrm{u},\nu}\big|^{\max}_{\mathrm{c},\nu}}{\sigma_s^4} \quad (15)$$

when the Wiener symbol estimator satisfies the UMSE condition $J_{\mathrm{u},\nu}(\boldsymbol{q}_{\mathrm{m},\nu})\le J_{\mathrm{o}}\sigma_s^2$ in Theorem 1.

Proof: To ensure that our bound applies to both finite and infinite-dimensional channels and estimators, we introduce the following operator:

$$\boldsymbol{\mathcal{H}}_M : \ell_1(\mathbb{C}^P)\to\mathbb{C}^{PQ} \text{ s.t.}$$

$$\boldsymbol{\mathcal{H}}_M\,\boldsymbol{q} \;=\; \begin{pmatrix} \sum_{k,i}\mathbf{h}^{(k)}_{i+M}q^{(k)}_i \\ \sum_{k,i}\mathbf{h}^{(k)}_{i+M-1}q^{(k)}_i \\ \vdots \\ \sum_{k,i}\mathbf{h}^{(k)}_{i+M-Q}q^{(k)}_i \end{pmatrix}.$$

Recall that $\boldsymbol{q}$ and $\ell_1(\mathbb{C}^P)$ were defined in Section 2.1. When $\mathbf{h}^{(k)}(z)$ are FIR, $\boldsymbol{\mathcal{H}}_M$ reduces to a block Toeplitz matrix. The operator $\bar{\boldsymbol{\mathcal{H}}}_M$ will also prove useful:

$$\bar{\boldsymbol{\mathcal{H}}}_M : \ell_1(\mathbb{C}^P)\to\mathbb{C}^{PQ} \text{ s.t.}$$

$$\bar{\boldsymbol{\mathcal{H}}}_M\,\bar{\boldsymbol{q}} \;=\; \begin{pmatrix} \sum_{(k,i)\neq(0,\nu)}\mathbf{h}^{(k)}_{i+M}q^{(k)}_i \\ \sum_{(k,i)\neq(0,\nu)}\mathbf{h}^{(k)}_{i+M-1}q^{(k)}_i \\ \vdots \\ \sum_{(k,i)\neq(0,\nu)}\mathbf{h}^{(k)}_{i+M-Q}q^{(k)}_i \end{pmatrix}.$$

$\bar{\boldsymbol{\mathcal{H}}}_M$ is a version of $\boldsymbol{\mathcal{H}}_M$ with the components for the 0^{th} source at delay ν removed, and $\bar{\boldsymbol{q}}$ is a version of $\boldsymbol{q}$ with the $q^{(0)}_\nu$ element extracted.

Using (12) and the definitions of $\hat{\boldsymbol{h}}^{(0)}_{\nu+M}$ and $\boldsymbol{h}^{(0)}_{\nu+M}$ in (14), the operators $\boldsymbol{\mathcal{H}}_M$ and $\bar{\boldsymbol{\mathcal{H}}}_M$ allow us to write

$$\hat{\boldsymbol{h}}^{(0)}_{\nu+M} \;=\; \boldsymbol{\mathcal{H}}_M\,\boldsymbol{q}^*\sigma_s^2 \;=\; \bar{\boldsymbol{\mathcal{H}}}_M\,\bar{\boldsymbol{q}}^*\sigma_s^2 + \boldsymbol{h}^{(0)}_{\nu+M}q^{(0)*}_\nu\sigma_s^2.$$

Choosing $\theta=(q^{(0)*}_\nu\sigma_s^2)^{-1}$ in (14),

$$\mathcal{E}_{\hat{\boldsymbol{h}}} \le \frac{1}{Q+1}\left\|\frac{\hat{\boldsymbol{h}}^{(0)}_{\nu+M}}{q^{(0)*}_\nu\sigma_s^2}-\boldsymbol{h}^{(0)}_{\nu+M}\right\|_2^2 = \frac{1}{Q+1}\frac{\left\|\bar{\boldsymbol{\mathcal{H}}}_M\,\bar{\boldsymbol{q}}^*\right\|_2^2}{|q^{(0)}_\nu|^2}. \quad (16)$$

The induced norm $\|\boldsymbol{\mathcal{H}}_M\| := \sup_{\boldsymbol{q}\neq\boldsymbol{0}}\|\boldsymbol{\mathcal{H}}_M\,\boldsymbol{q}^*\|_2/\|\boldsymbol{q}\|_2$ (which, for finite-dimensional $\boldsymbol{\mathcal{H}}_M$, equals the largest singular value) allows further bounding of (16):

$$\mathcal{E}_{\hat{\boldsymbol{h}}} \;\le\; \frac{1}{Q+1}\frac{\|\bar{\boldsymbol{\mathcal{H}}}_M\|^2\|\bar{\boldsymbol{q}}\|_2^2}{|q^{(0)}_\nu|^2} \;=\; J_{\mathrm{u},\nu}(\boldsymbol{q}_{\mathrm{c},\nu})\,\frac{\|\bar{\boldsymbol{\mathcal{H}}}_M\|^2}{(Q+1)\sigma_s^2}. \quad (17)$$

When $\{\mathbf{h}^{(k)}(z)\}$, $\mathcal{Q}_{\mathrm{a}}$, and ν are such that $J_{\mathrm{u},\nu}(\boldsymbol{q}_{\mathrm{m},\nu})\le J_{\mathrm{o}}\sigma_s^2$ for J_{o} in (10), Theorem 1 allows upper bounding of $J_{\mathrm{u},\nu}(\boldsymbol{q}_{\mathrm{c},\nu})$ and (17) becomes

$$\mathcal{E}_{\hat{\boldsymbol{h}}} \;\le\; J_{\mathrm{u},\nu}\big|^{\max}_{\mathrm{c},\nu}\,\frac{\|\bar{\boldsymbol{\mathcal{H}}}_M\|^2}{(Q+1)\sigma_s^2}. \quad (18)$$

Since $\|\boldsymbol{\mathcal{H}}_M\|^2=\sup_{\|\boldsymbol{q}\|_2=1}\boldsymbol{q}^t\boldsymbol{\mathcal{H}}_M^H\boldsymbol{\mathcal{H}}_M\,\boldsymbol{q}^*\ge \sup_{\|\boldsymbol{q}\|_2=1,\,q^{(0)}_\nu=0}\boldsymbol{q}^t\boldsymbol{\mathcal{H}}_M^H\boldsymbol{\mathcal{H}}_M\,\boldsymbol{q}^*=\sup_{\|\bar{\boldsymbol{q}}\|_2=1}\bar{\boldsymbol{q}}^t\bar{\boldsymbol{\mathcal{H}}}_M^H\bar{\boldsymbol{\mathcal{H}}}_M\,\bar{\boldsymbol{q}}^*=\|\bar{\boldsymbol{\mathcal{H}}}_M\|^2$, (18) yields

$$\mathcal{E}_{\hat{\boldsymbol{h}}} \;\le\; J_{\mathrm{u},\nu}\big|^{\max}_{\mathrm{c},\nu}\,\frac{\|\boldsymbol{\mathcal{H}}_M\|^2}{(Q+1)\sigma_s^2}. \quad (19)$$

Simplification of (19) is possible using the fact that $\|\boldsymbol{\mathcal{H}}_M\,\boldsymbol{q}^*\|_2^2\le(Q+1)\sum_{k,i}\|\mathbf{h}^{(k)}_i\|_2^2\,\|\boldsymbol{q}\|_2^2$ which implies

$$\|\boldsymbol{\mathcal{H}}_M\|^2 \;\le\; (Q+1)\sum_{k,i}\|\mathbf{h}^{(k)}_i\|_2^2. \quad (20)$$

Rewriting (20) using

$$\sum_{k,i}\|\mathbf{h}^{(k)}_i\|_2^2=\frac{1}{\sigma_s^2}\mathrm{E}\left\{\left\|\sum_{k,i}\mathbf{h}^{(k)}_i s^{(k)}_{n-i}\right\|_2^2\right\}=\frac{1}{\sigma_s^2}\mathrm{E}\left\{\|\mathbf{r}_n\|_2^2\right\}$$

gives $\|\boldsymbol{\mathcal{H}}_M\|_2^2\le\frac{Q+1}{\sigma_s^4}\mathrm{E}\left\{\|\mathbf{r}_n\|_2^2\right\}$, which leads to

$$\mathcal{E}_{\hat{\boldsymbol{h}}} \;\le\; \frac{1}{\sigma_s^4}J_{\mathrm{u},\nu}\big|^{\max}_{\mathrm{c},\nu}\,\mathrm{E}\left\{\|\mathbf{r}_n\|_2^2\right\}. \quad (21)$$

■

Theorem 2 gives an upper bound for the ASPE that is proportional to the norm of the channel operator and the UMSE of ν-delayed Wiener symbol estimators (via $J_{\mathrm{u},\nu}\big|^{\max}_{\mathrm{c},\nu}$ in (11)), as well as a looser bound that is proportional to the received power and the Wiener UMSE.

3.2 ASPE with Correlation Approximation

In practice, the expectation operations in Fig. 2 will be replaced by some sort of block or exponential averages. In this section, we analyze the effect of block averaging on the parameter estimation error. The δ^{th} block parameter estimate is defined below for block size N.

$$\hat{\mathbf{h}}^{(0)}_{\nu+M-\delta} \;:=\; \frac{1}{N}\sum_{n=0}^{N-1} \mathbf{r}_{n-\delta} y^*_{n-M}. \tag{22}$$

Lemma 1 (See [5] for proof.) *The expected ASPE using N-block correlation estimates can be written*

$$\mathrm{E}\{\mathcal{E}_{\hat{\hat{\boldsymbol{h}}}}\} \;=\; \mathcal{E}_{\hat{\boldsymbol{h}}} + \frac{\sigma_s^4}{N(Q+1)} \frac{|\hat{\boldsymbol{h}}^{(0)H}_{\nu+M}\boldsymbol{h}^{(0)}_{\nu+M}|^2}{\left\|\sum_{k,i}\sqrt{\kappa_s^{(k)}-1}\,\mathbf{h}^{(k)}_{i+M-\delta}q_i^{(k)*}\right\|_2^2 + \|\hat{\boldsymbol{h}}^{(0)}_{\nu+M}\|_2^4} \sum_{\overline{k}\neq 0}^{Q} \mathbf{h}^{(k)H}_{\overline{k}} \mathbf{h}^{(\overline{k})}_{j+p} \sum_{\substack{(\ell,i)\neq \\ (k,j+M-\delta)}} \cdots q_i^{(\ell)} q_{i+p}^{(\ell)*}\Big). \tag{23}$$

Simulations suggest that, for CM-minimizing estimators $\mathbf{f}_{\mathrm{c},\nu}(z)$ and typical values of N, the second term in (23) dominates the first. This implies that the performance of the proposed channel estimation scheme is in practice limited by the finite-data correlations rather than by the performance of the blind symbol estimates. The plots in Section 4 agree with this notion: improvement in symbol estimates gained through quantization of $\{y_n\}$ gives the Gooch-Harp scheme [7] only minor advantage in ASPE.

4.0 Numerical Examples

Figs. 4 and 5 each plot bounds (19) and (21) for the ASPE of the exact CM-minimizing estimator with exact cross-correlations compared to (i) the average ASPE achieved using CMA-derived estimates and block length $N = 10^4$, (ii) the average ASPE achieved by the Gooch-Harp scheme [7] using block length N, (iii) the expected ASPE for the exact CM-minimizing estimator[2] using block length N (from (23)), and (iv) the ASPE for the exact CM-minimizing estimator with exact cross-correlations (13).

Fig. 4 is based on a complex-valued $T/2$-spaced (i.e., $P = 2$) SPIB[3] microwave channel response model #3, shortened to a 16 symbol duration, in various levels of AWGN. The impulse response of channel #3 is shown in Fig. 6(a)-(b) and example channel estimation errors are plotted in Fig. 6(c)-(d). The complex-valued $T/2$-spaced equalizer $\mathbf{f}(z)$ had a time support of 10 symbols. Fig. 5 is based on SPIB channel #2 and a number of different restrictions on symbol estimator length N_f. The impulse response of channel #2 is shown in Fig. 7(a)-(b) and example channel estimation errors are plotted in Fig. 7(c)-(d). The SNR of AWGN was 40 dB.

The following were common to all experiments: the desired source was i.i.d. and drawn from a 64-QAM alphabet; ν was the MSE-minimizing symbol delay for the particular combination of channel, noise, and equalizer constraints; Q and M were adjusted so that all 32 $T/2$-spaced coefficients of the SPIB channel were estimated; and CMA was initialized at $\mathbf{f}_{\mathrm{c},\nu}(z)$ and adapted with stepsize $\mu = 10^{-3}$.

The fact that the upper-bound-(19) trace crosses the N-block traces in Figs. 4 and 5 should not cause alarm: (19) bounds the ASPE assuming *exact* cross-correlations, while the CMA, Gooch-Harp, and CM-N traces assume length-N block approximations of the cross-correlations.

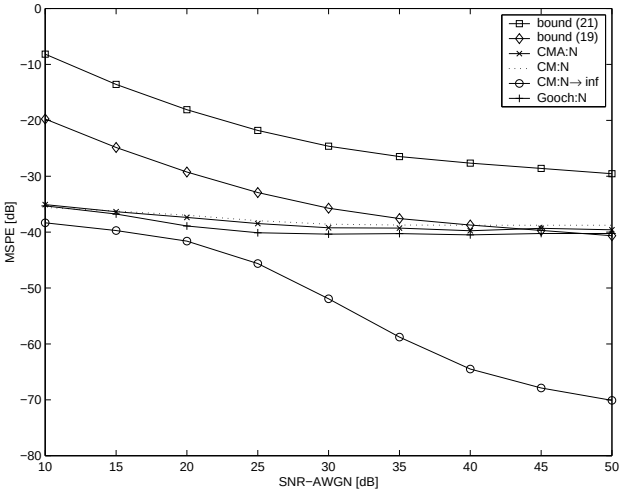

Fig. 4. ASPE for 32-tap $T/2$-spaced SPIB microwave channel #3 versus SNR w.r.t. AWGN.

5.0 Conclusions

We have analyzed the performance of a blind channel identification scheme based on the cross-correlation of CM-minimizing blind symbol estimates with the received signal. Leveraging recent bounds on the UMSE of CM-minimizing symbol estimates, upper bounds on the average squared channel parameter estimation error (ASPE) were derived. The ASPE increase due to finite-data correlator approximation was also examined, and experiments using SPIB microwave channel models were presented to verify the results of our analyses.

[2]The CM-minimizing estimator $\mathbf{f}_{\mathrm{c},\nu}(z)$ was determined numerically using Matlab's "fminunc" routine.

[3]The SPIB microwave channel database resides at `http://spib.rice.edu/spib/microwave.html`.

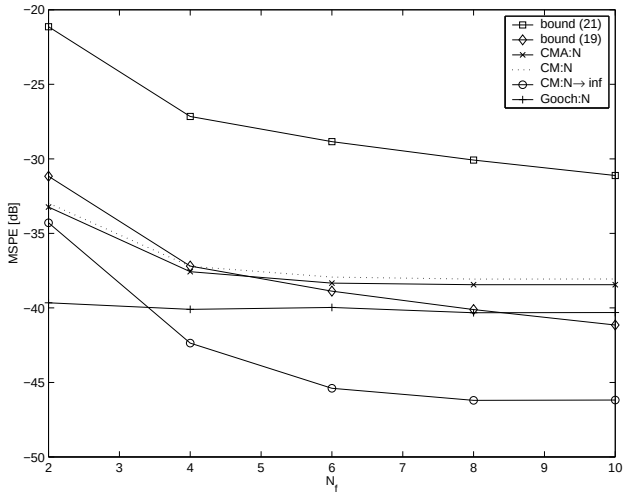

Fig. 5. ASPE for 32-tap $T/2$-spaced SPIB microwave channel #3 versus symbol estimator length N_f.

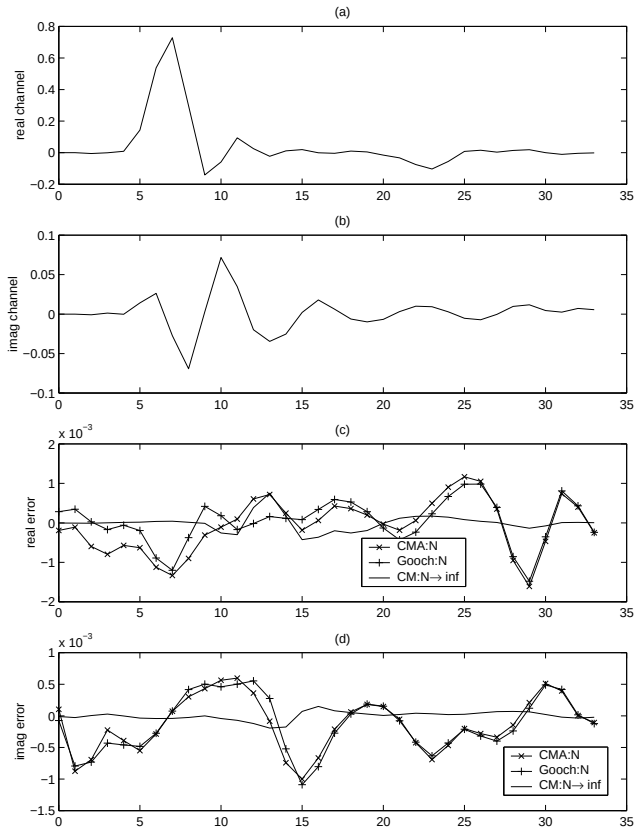

Fig. 6. (a) Real and (b) imaginary components of 32-tap $T/2$-spaced SPIB microwave channel #3 impulse response. (c) Real and (d) imaginary components of estimation errors for SNR = 50 dB and $N_f = 10$.

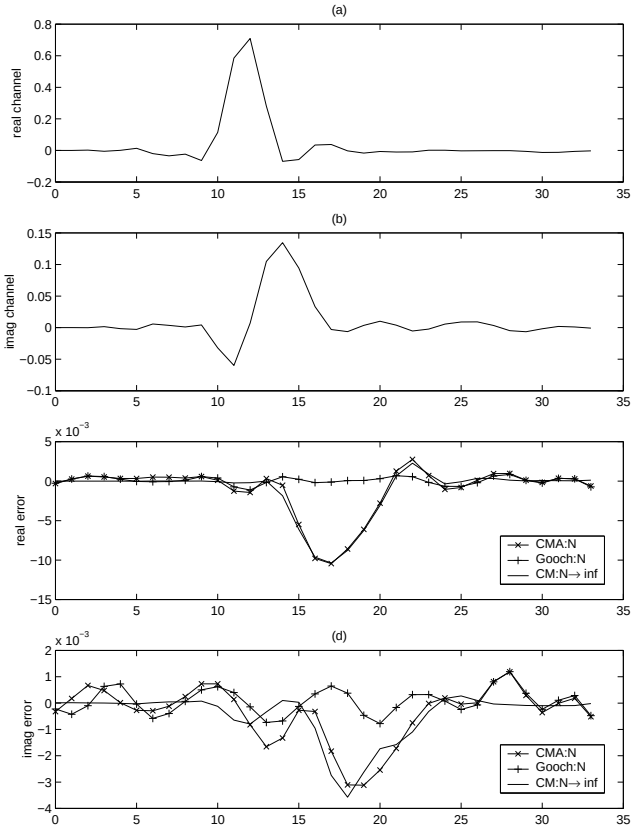

Fig. 7. (a) Real and (b) imaginary components of 32-tap $T/2$-spaced SPIB microwave channel #2 impulse response. (c) Real and (d) imaginary components of estimation errors for SNR = 40 dB and $N_f = 10$.

6.0 References

[1] L. Tong and S. Perreau, "Blind channel estimation: From subspace to maximum likelihood methods," *Proc. IEEE*, vol. 86, no. 10, pp. 1951-68, Oct. 1998.

[2] D.N. Godard, "Self-recovering equalization and carrier tracking in two-dimensional data communication systems," *IEEE Trans. Comm.*, vol. 28, no.11, pp. 1867-75, Nov. 1980.

[3] J.R. Treichler and B.G. Agee, "A new approach to multipath correction of constant modulus signals," *IEEE Trans. Acoust., Speech, and Signal Processing*, vol. ASSP-31, no.2, pp. 459-72, Apr. 1983.

[4] C.R. Johnson, Jr., P. Schniter, T.J. Endres, J.D. Behm, D.R. Brown, and R.A. Casas, "Blind equalization using the constant modulus criterion: A review," *Proc. IEEE*, vol. 86, no. 10, pp. 1927-50, Oct. 1998.

[5] P. Schniter, R. Casas, A. Touzni, and C.R. Johnson, Jr., "Performance analysis of Godard-based blind channel identification," submitted to *IEEE Trans. on Signal Processing*, Sept. 1999.

[6] P. Schniter and C.R. Johnson, Jr., "Bounds for the MSE performance of constant modulus estimators," to appear in *IEEE Trans. Inform. Theory*, 2000.

[7] R.P. Gooch and J.C. Harp, "Blind channel identification using the constant modulus adaptive algorithm," in *Proc. IEEE Internat. Conf. Comm.* (Philly, PA), pp. 75-9, 1988.